Optical Materials 35 (2013) 1455–1460

Contents lists available at SciVerse ScienceDirect

Optical Materials

journal homepage: www.elsevier.com/locate/optmat

Unidirectional light propagation characters of the triangular-lattice hybrid-waveguide photonic crystals

Shuai Feng *, Yiquan Wang

School of Science, Minzu University of China, Beijing 100081, China

ARTICLE INFO

Article history:
Received 28 December 2012
Received in revised form 11 February 2013
Accepted 28 February 2013
Available online 25 March 2013

Keywords:
Photonic crystal
Unidirectional light propagation
Waveguide
Mode conversion

ABSTRACT

The high-contrast unidirectional light transport through the two-dimensional triangular-lattice photonic crystal structures is numerically studied by the finite-difference time-domain method. Through utilizing the modal match and mismatch of the waveguides to the incident light beams, and adjusting the coupling region connecting the two waveguides with different symmetric guiding modes, the unidirectional light propagation for the fundamental even-symmetric light beam is achieved. And the unidirectional light beam propagations within two different wavelength regions along the same and opposite directions are both obtained through the optimized hybrid-waveguide structures. The influence of the air holes' radius disorder existing inevitably in the actual fabrication process to the unidirectional light transport character of the proposed structures is also studied.

1. Introduction

Photonic crystals (PCs) [1,2] are a novel class of optical media with very interesting characters and a large variety of applications. A lot of devices based on PCs have been proposed, such as waveguides, beam splitters, filters, and super prisms. Owing to the easy fabrication and convenient integration with other conventional devices, the two-dimensional (2D) PC devices play the potential important functions in the future all-optical integrated circuits [3–6]. It is well known that the electrical diode plays an important role in electronic circuits owing to its capability of unidirectional movement of the current flux. An all-optical diode is a spatially nonreciprocal device that offers unidirectional propagation of light beams, which plays key roles in the all-optical integrated circuits.

The efficient routines to breaking the reciprocity or time-reversal symmetry and obtaining the unidirectional light propagation are based on magnetic-optical effect [7,8], optical nonlinearity [9,10], opto-acoustic effect [11,12]. Wang et al. [13] designed a unidirectional on-chip optical diode in silicon based on the directional band gap difference of the near-infrared square-lattice PCs comprising a heterojunction structure and the break of the spatial inversion symmetry. Feng et al. [14] obtained a one-way modal conversion effect through a two-mode waveguide with a spatially varying but time-independent dielectric constant both numerically and experimentally. Fan et al. [15] showed that the structure proposed in [14] cannot enable optical isolation because it possesses a symmetric scattering matrix. And an optical isolator cannot be constructed by incorporating this structure into any linear and time-independent system, which is described by materials with a scalar dielectric function. In the past two years, a great deal of efforts has been dedicated to studying the unidirectional propagation of the electromagnetic waves in the linear and passive PCs [16–25]. Miller [22] showed that every linear optical component can be completely described as a device that converts one set of orthogonal input modes to a matching set of orthogonal output modes, so all the linear optical devices are mode converts. For the incident light beam with a particular modal symmetry, the unidirectional propagation through a linear devices can be obtained and the output light beam is converted to be different modal-symmetric, which has potential applications in the complex integrated circuits. Wang et al. [23] demonstrated the optical isolation of infrared light in purely linear and passive silicon photonic structures both theoretically and experimentally, which is attributed to the information dissipation due to off-plane and side-way scattering and selective modal conversion in the multiple-channel structure and has no conflict with the reciprocal principle.

In this paper, we studied the unidirectional propagation characters of the fundamental even-symmetric light beams through a hybrid-waveguide PC structure, where the two waveguides have different modal symmetries within the same wavelength region. Owing to the match and mismatch of the guiding modes' symmetries to the input fundamental even-symmetric light signals, and the mode conversion characters from one waveguide to another, it is obtained that the unidirectional high-contrast near-infrared light transport within two different wavelength regions along the same and opposite directions through optimizing the hybrid-waveguide structures.

* Corresponding author. Tel.: +86 1068932205.
E-mail address: fengshuai75@163.com (S. Feng).

0925-3467/$ - see front matter
http://dx.doi.org/10.1016/j.optmat.2013.02.020

2. Unidirectional light propagation through hybrid-waveguide structures

Firstly, we consider a PC structure consisting of a triangular lattice of air holes embedded in the silicon background, whose refractive index is set to be 3.45 for the near-infrared light around 1550 nm. In our simulation, the length of the PC's lattice constant "a" is defined to be 400 nm, and the radius of the air holes is set to be 140 nm. It is calculated that there exists a TE-polarized photonic band gap between the wavelengths of 1216 nm and 1810 nm. Based on above PC, we constructed a waveguide by removing a row of air hole along the Γ–*K* direction of the PC. The calculated guiding bands are shown in Fig. 1a by the solid dot lines for the even modes and the hollow dot lines for the odd modes. When the waveguide is constructed by removing a row of air holes along the Γ–*M* direction of the PC, the calculated results are shown in Fig. 1b, which indicates that the width of the even-mode guiding band centered around 1550 nm decreases apparently comparing to the W1-typed Γ–*K* directional waveguide. And the wavelength regions of the odd-mode guiding bands in above two waveguides are both contained by those of the even-mode guiding bands. Based on the W1-typed Γ–*M* directional waveguide, we reduced the radius of air holes in the nearest two rows from 140 nm to 80 nm, whose sketch map is shown in Fig. 2a as the under waveguide. The corresponding calculated guiding bands for this waveguide is shown in Fig. 1c, where a more number of even-mode and odd-mode guiding bands appear within the band gap of the PC.

Based on the two waveguides whose guiding bands are shown in Fig. 1a and c, we constructed a kind of hybrid-waveguide structure shown in Fig. 2a. When a fundamental-mode light beam is incident from the left waveguide of the structure, the transmitted spectrum collected at the bottom of the under waveguide is shown by the solid line in Fig. 2b, while the reversed transmitted spectrum propagating from the under waveguide to the left waveguide is shown by the dotted line. It is obvious that there is a unidirectional light propagation phenomenon within the wavelength region existing from 1587 nm to 1660 nm, except that there is a sharp transmission drop around 1652 nm. The corresponding transmission contrasts are more than 10,000 with a maximum about 500,000, which is defined as the ratio of maximum transmittance in one direction to the corresponding transmittance in the reverse direction. Based on the structure shown in Fig. 2a, we added an air hole at the corner of the two waveguides, whose sketch map is depicted in Fig. 2c, and the corresponding calculated transmission spectra are shown in Fig. 2d. Comparing to Fig. 2b, it can be seen that the sharp transmission drop around 1645 nm disappears, and another unidirectional propagating wavelength region appears from 1408 nm to 1455 nm, where the transmission contrasts are more than 100 with a maximum about 280,000 at 1440 nm.

In order to have a visual sight of the propagation characteristics of the light waves through the above structure, the spatial magnetic field distributions of the upward and leftward fundamental-mode light beams at the wavelengths of 1600 nm and 1440 nm are calculated and the results are shown in Fig. 3. In Fig. 3a, the light wave resonant at 1600 nm cannot go upward through the under waveguide owing to even-mode band gap. When the light beam at the same wavelength is incident from the left waveguide, it is shown in Fig. 3b that the light beam can propagate through the left waveguide, and an odd-mode light beam is converted in the waveguide below. Finally the light beam is released at the output port of the waveguide below. When the wavelength of the light beam is changed to be 1440 nm, Fig. 3c shows that the light beam launched at the bottom of the under waveguide can propagate upwards, but no light beam is converted into the left waveguide.

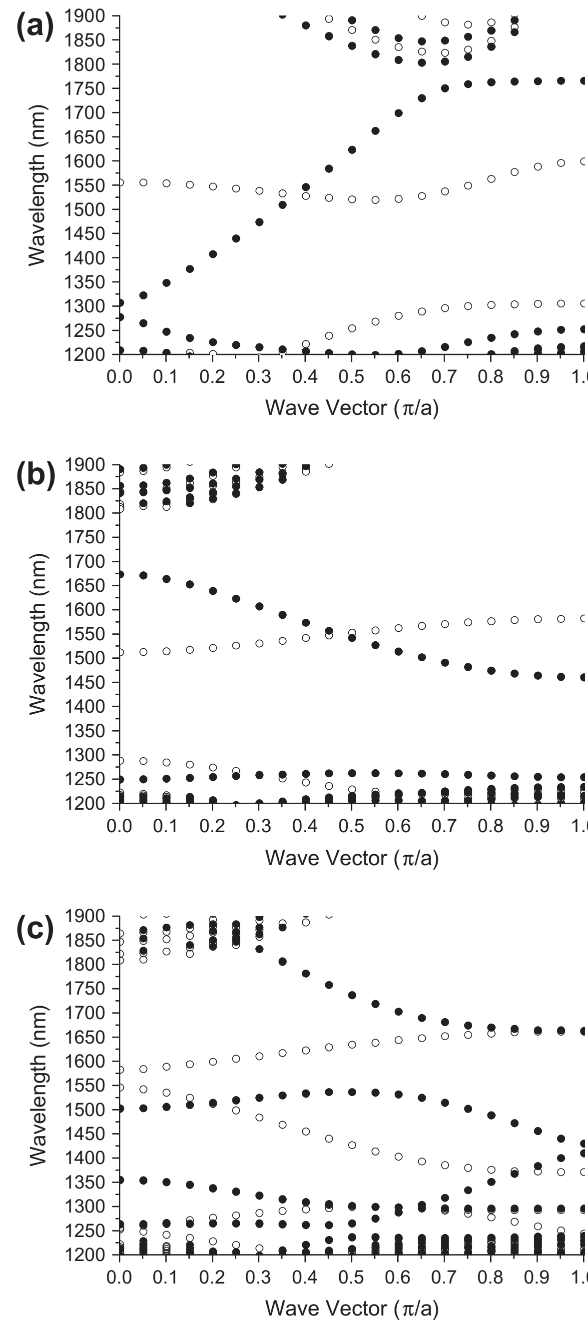

Fig. 1. Calculated even-mode guiding bands (shown by the solid dots), and odd-mode guiding bands (shown by the hollow dots) in three waveguides. The length of the PC's lattice constant is 400 nm, the radius of the air rods is 140 nm, and the refractive index of the silicon background is 3.45. (a) The W1-typed waveguide along the Γ-K direction, (b) the W1-typed waveguide along the Γ–*M* direction, (c) the Γ–*M* directional waveguide constructed by removing a row of air holes and reducing the radius of the air holes in the two adjacent rows from 140 nm to 80 nm.

Fig. 3d shows that the light beam resonant at 1440 nm can travel along the left waveguide, and is converted to an odd-mode light beam propagating downwards in the under waveguide. Comparing Fig. 3a with Fig. 3c, it is found that there is an apparent difference in the phenomena of preventing light's propagation from the under waveguide. The first is utilizing the even-mode band gap for the incident fundamental-mode light beam, while the second is through the no coupling of the light beam from one waveguide to another.

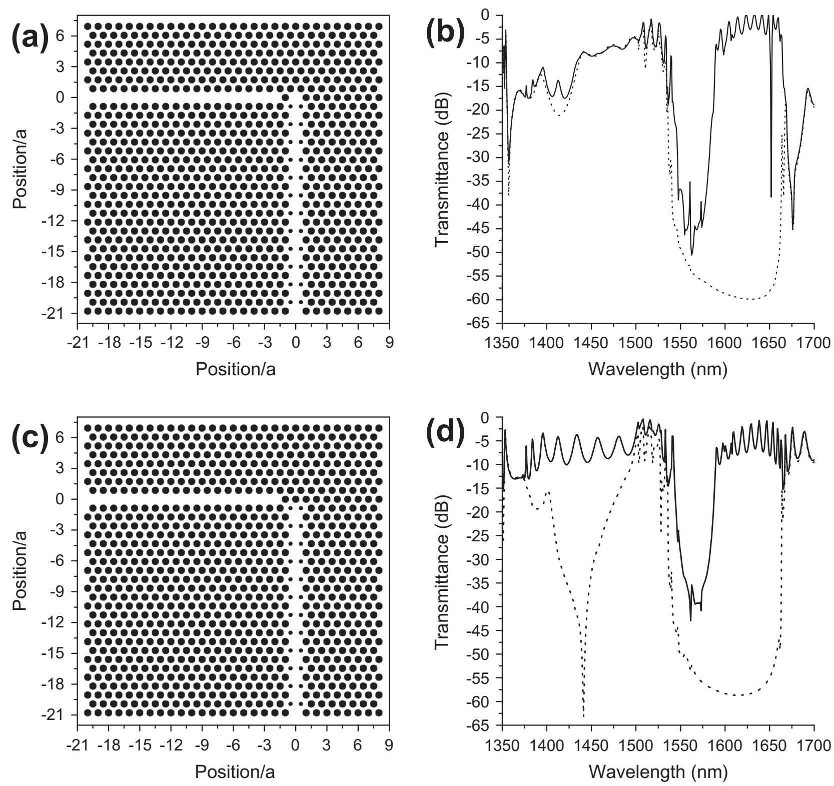

Fig. 2. (a) Sketch map of a 2D triangular-lattice PC structure consisting of two kinds of waveguides, (b) transmittances of a fundamental-mode light beam propagating through the structure shown in (a), which is incident from the left side (shown by the solid line) and under (shown by the dotted line) of the structure with a spatial beam width of 800 nm, (c) the same as (a) except that an air hole is added at the corner of the two waveguides, (d) the same as (b) except that is for the structure (c).

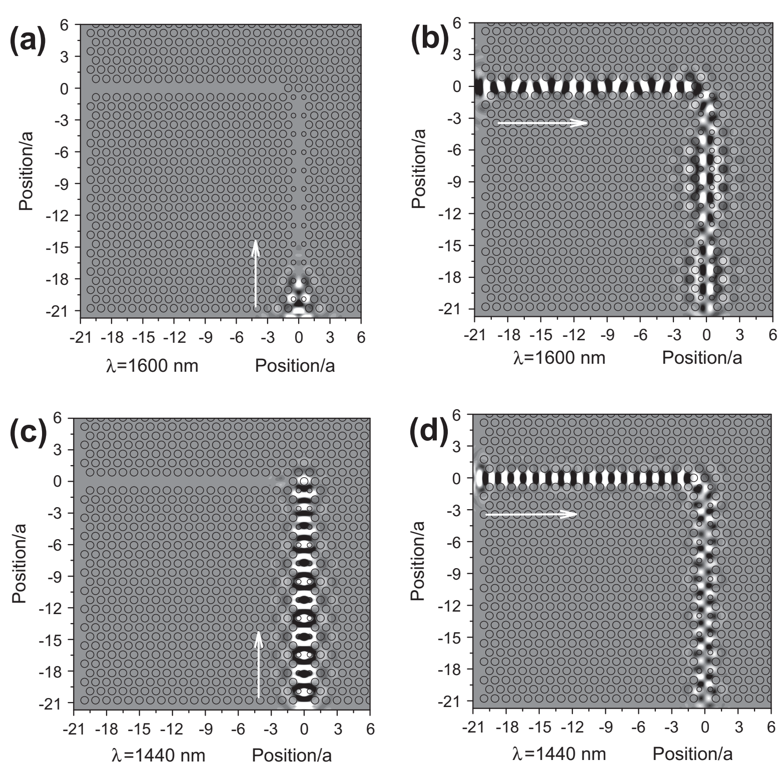

Fig. 3. Spatial distributions of magnetic field through the structure shown in Fig. 2c at fundamental-mode normal incidence of the light sources with different wavelengths. The arrows point at the directions of light propagation through the structure. (a) 1600 nm at upward incidence, (b) 1600 nm at rightward incidence, (c) 1440 nm at upward incidence, (d) 1440 nm at rightward incidence. White and black regions represent the positive and negative values of the magnetic field, respectively.

In above hybrid-waveguide structures, the forward light propagation direction is vertical to the backward light transport direction. Based on one of above waveguides, we designed another kind of unidirectional propagation device whose sketch map is shown in Fig. 4a. The banding structure of the left W1-typed Γ–*M* directional waveguide is shown in Fig. 1b, while that of the right waveguide shown in Fig. 4a is described in Fig. 1c. Comparing Fig. 1b with Fig. 1c, we can see that the wavelengths between 1581 nm and 1660 nm are within the even-symmetric guiding band shown in Fig. 1b, while they are also within the odd-symmetric guiding band shown in Fig. 1c. For the wavelengths between 1262 nm and 1290 nm, the situations are just opposite. The connecting region between above two waveguides is designed by interlacing one air hole with different radius, which can attribute to the modal conversion of the incident light beam from one waveguide to the other. Fig. 4c shows the light transmittances through the hybrid-waveguide structure at the normal incidence from the left (shown by the dotted line) and right (shown by the solid line) sides of the structure shown in Fig. 4a. It is shown that two unidirectional propagation wavelength regions exist. The maxima of the transmission contrasts in above two wavelength regions are both more than 100,000. There also exist two sharp transmission drops centred at the wavelengths of 1286 nm and 1621 nm within above two wavelength regions, respectively. To diminish these two sharp transmission drops, we optimized the structure by interlacing two air holes with different radius in the coupling region, whose sketch map is shown in Fig. 4b. Fig. 4d shows that corresponding calculated transmittances through the optimized structure, where the two sharp drops disappear apparently. The spatial magnetic field distributions of the leftward and rightward light beam resonant at the wavelengths of 1600 nm and 1290 nm through above structure are calculated and the results are shown in Fig. 5. In Fig. 5a, the fundamental-mode light beam incident from the left side and resonant at 1600 nm goes straight in the left waveguide, and it is transformed into an odd-mode light beam in the right waveguide. When the same light beam is incident from the right side of the structure, Fig. 5b shows that no light energy can reach the left waveguide owing to the even-mode guiding band gap of the right waveguide structure. When the incident light's wavelength is changed from 1600 nm to 1290 nm, the propagating characters are just opposite, as is shown in Fig. 5c and d.

Considering the structure disorders existing inevitably in the actual fabrication process, we calculated the influence of air holes' radius disorder on the unidirectional light propagation characteristics. A random function is introduced to describe the holes' size, and the calculated results show that the unidirectional propagation characters of above structures are very sensitive to the variation of the air hole's radius. To ensure the apparent unidirectional propagation characteristics, the structure shown in Fig. 3c can tolerate a maximum deviation from the original values of 10% degree, while that in Fig. 4b can only tolerate a maximum of 5% degree. These simulated results provide good suggestions to the actual fabrication and utilization of unidirectional propagating devices in the all-optical integrated circuits.

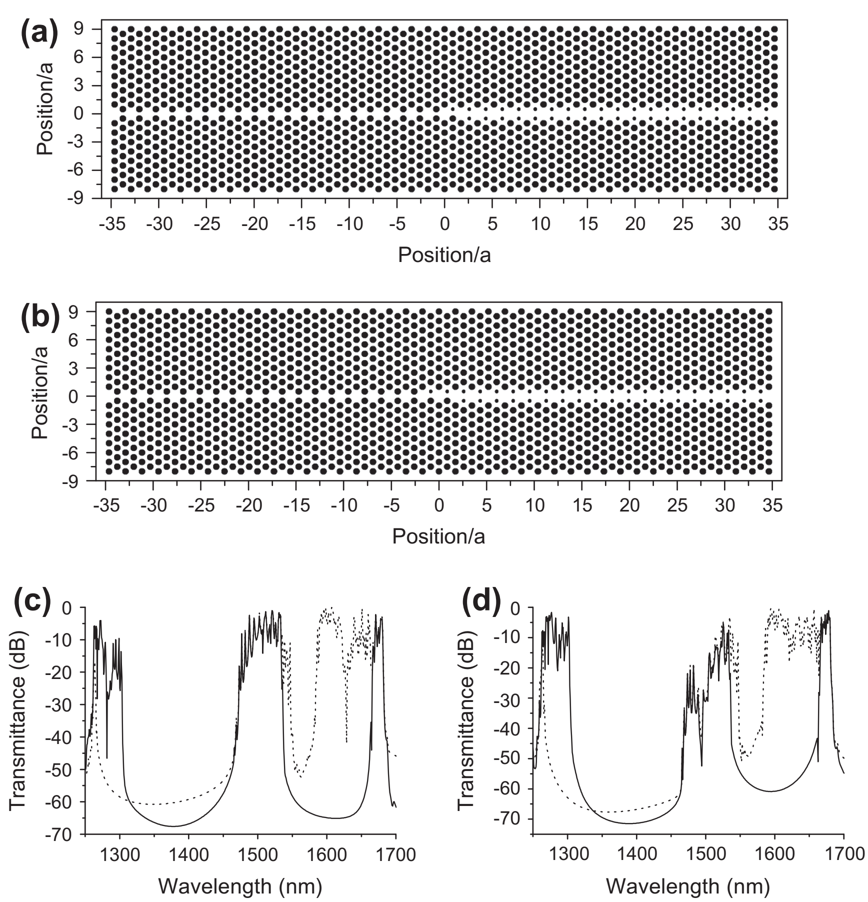

Fig. 4. Sketch maps of the unidirectional-propagating hybrid-waveguide structures constructed by interlacing one (a) and (b) two air holes with different radiuses. And light transmittances (c) and (d) through the structures (a) and (b) from a fundamental-mode light beam at the normal incidence from the left (shown by the dotted line) and right (shown by the solid line) sides of the waveguide, respectively.

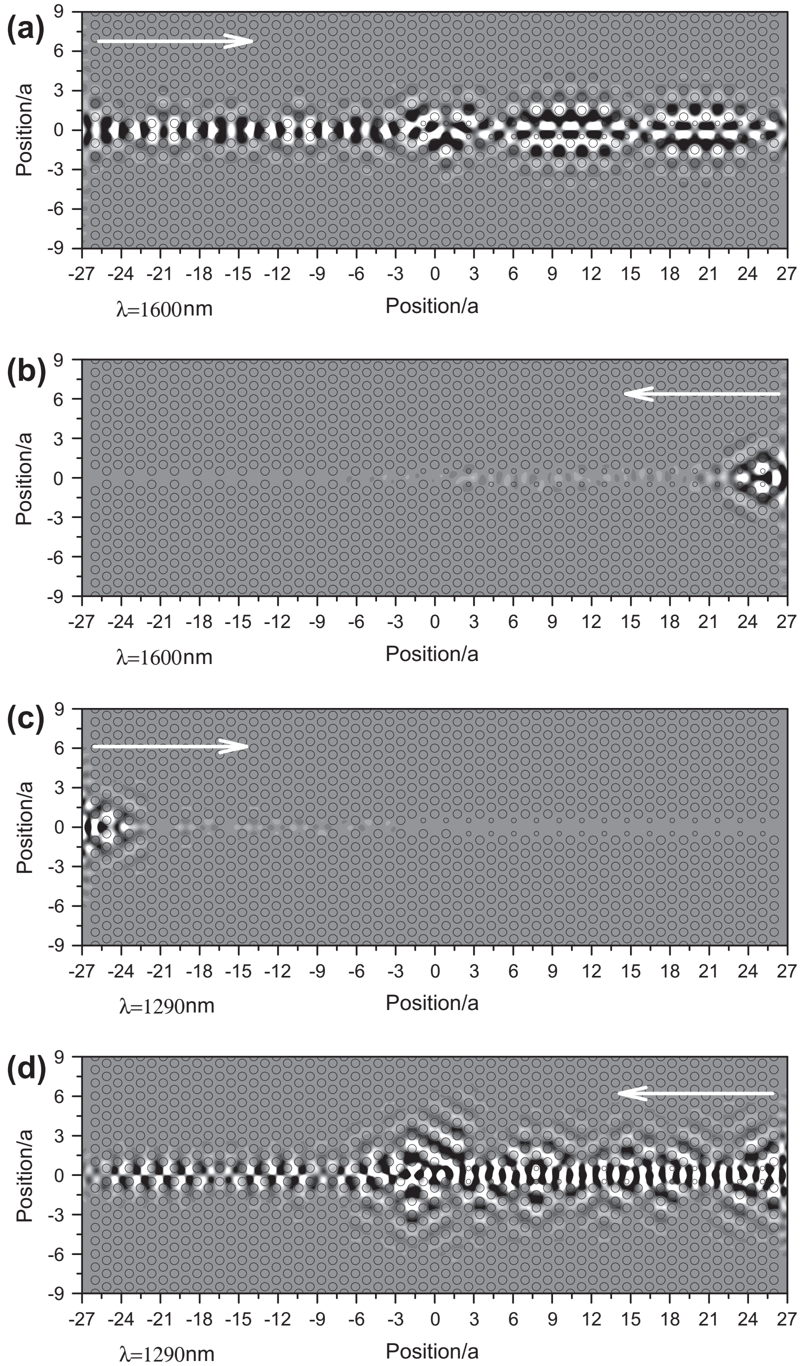

Fig. 5. Spatial distributions of magnetic fields at the wavelengths of 1600 nm and 1290 nm through the structure shown in Fig. 4b at normal incidence of fundamental-mode light source. The arrows point at the directions of light propagation through the structure. (a) 1600 nm at rightward incidence, (b) 1600 nm at leftward incidence, (c) 1290 nm at rightward incidence, (d) 1290 nm at leftward incidence. White and black regions represent the positive and negative values of the magnetic field, respectively.

3. Summary

In conclusion, the unidirectional fundamental-mode light propagation through the 2D triangular-lattice hybrid-waveguide PC structures is studied in this paper. Based on the modal match and mismatch of the waveguides to the incident light beams, and the light beam's mode conversion at the connecting region of two waveguides with different modes' symmetries, the unidirectional light propagation for the foundational-mode light beams is achieved, and the output light beam is second-higher odd symmetric owing to the modal conversion in the coupling region between two waveguides. And the influence of the air holes' radius disorder to the structure's unidirectional light propagation is also studied. We know that there is a growing interest utilizing multiple spatial modes in optical systems to increase information processing capacity, including the fields of the fiber optic communications and on-chip optical integration. And this kind of unidirectional propagation device can control the light propagation within the waveguides. So it is more suitable to connect with other optical devices and has potential important applications in the complex all-optical integrated circuits.

Acknowledgements

This work was supported by the National Natural Science Foundation of China with Grant no. 10904176, and the "985 Project" of the Ministry of Education of China.

References

[1] E. Yablonovitch, Phys. Rev. Lett. 58 (1987) 2059–2062.
[2] S. John, Phys. Rev. Lett. 58 (1987) 2486–2489.
[3] M. Tokushima, H. Kosaka, A. Tomita, H. Yamada, Appl. Phys. Lett. 76 (2000) 952.
[4] M. Notomi, K. Yamada, A. Shinya, J. Takahashi, C. Takahashi, I. Yokohama, Phys. Rev. Lett. 87 (2001) 253902.
[5] S. Noda, A. Chutinan, M. Imada, Nature 407 (2002) 608–610.
[6] B.S. Song, S. Noda, T. Asano, Sci. 300 (2003) 1537.
[7] Z. Yu, G. Veronis, Z. Wang, S. Fan, Phys. Rev. Lett. 100 (2008) 023902.
[8] Z. Wang, Y. Chong, J.D. Joannopoulos, M. Soljacic, Nature 461 (2009) 772–775.
[9] K. Gallo, G. Assanto, K.R. Parameswaran, M.M. Fejer, Appl. Phys. Lett. 79 (314) (2001) 1–3.
[10] M. Soljačić, C.Y. Luo, J.D. Joannopoulos, Opt. Lett. 28 (2003) 637–639.
[11] X.F. Li, X. Ni, L. Feng, M.H. Lu, C. He, Y.F. Chen, Phys. Rev. Lett. 106 (2011) 084301.
[12] Z. Yu, S. Fan, Nat. Photon. 3 (2009) 91–94.
[13] C. Wang, C.Z. Zhou, Z.Y. Li, Opt. Express 19 (2011) 26948–26955.
[14] L. Feng, M. Ayache, J. Huang, Y.L. Xu, M.H. Lu, Y.F. Chen, Y. Fainman, A. Scherer, Science 333 (2011) 729–733.
[15] S. Fan, R. Baets, A. Petrov, Z.F. Yu, John D. Joannopoulos, W. Freude, An. Melloni, M. Popović, M. Vanwolleghem, D. Jalas, M. Eich, M. Krause, H. Renner, E. Brinkmeyer, C.R. Doerr, Science 335 (2012) 38-b.
[16] M.S. Kang, A. Butsch, P.S.J. Russell, Nat. Photon. 5 (2011) 549–553.
[17] S. Feng, C. Ren, Y.Q. Wang, W.Z. Wang, EPL 97 (2012) 64001.
[18] A. Cicek, M.B. Yucel, O.A. Kaya, B. Ulug, Opt. Lett. 37 (2012) 2937–2939.
[19] C.C. Lu, X.Y. Hu, H. Yang, Q.H. Gong, Opt. Lett. 36 (2011) 4668–4670.
[20] S. Feng, W.Z. Wang, Y.Q. Wang, Jpn. J. Appl. Phys. 51 (2012) 112001.
[21] L. Fan, J. Wang, L.T. Varghese, H. Shen, B. Niu, Y. Xuan, A.M. Weiner, M.H. Qi, Science 335 (2012) 447–450.
[22] D.A.B. Miller, Opt. Express 20 (2012) 23985–23993.
[23] C. Wang, X.L. Zhong, Z.Y. Li, Sci. Rep. 2 (2012) 674.
[24] V. Liu, D.A.B. Miller, S.H. Fan, Opt. Express 20 (2012) 28388–28397.
[25] S. Feng, Y.Q. Wang, Opt. Express 21 (2013) 220–228.